



Waxpaper Actuator: Sequentially and Conditionally Programmable Wax Paper for Morphing Interfaces

Di Wu

wudi@cmu.edu

Human-Computer Interaction
Institute, Carnegie Mellon University
Pittsburgh, PA, USA

Emily Guan*

eguan12@pratt.edu

School of Architecture, Pratt Institute
Brooklyn, NY, USA
Human-Computer Interaction
Institute, Carnegie Mellon University
Pittsburgh, PA, USA

Yunjia Zhang*

yunjiaz@andrew.cmu.edu

Electrical and Computer Engineering,
Carnegie Mellon University
Pittsburgh, PA, USA

Hsuanju Lai

hsuanjul@andrew.cmu.edu
Electrical and Computer Engineering,
Carnegie Mellon University
Pittsburgh, PA, USA

Qiuyu Lu†

qiuyulu@berkeley.edu

Department of Mechanical
Engineering, University of California,
Berkeley
Berkeley, CA, USA

Lining Yao†

liningy@berkeley.edu

Department of Mechanical
Engineering, University of California,
Berkeley
Berkeley, CA, USA



Figure 1: Application demonstrations. (a) Seed Dispenser: Enables automated soil seeding in natural environments; (b) Morphing Flower: Features petals with varying gray levels that bloom sequentially; (c) Morphing Cicada: A laser-cut cicada toy with wings that morph sequentially; (d) Morphing Lampshade: Crafted from wax paper, responsive to spatial moisture; (e) Waxpaper Actuator as a Switch: Demonstrates versatility as an electrical circuit switch.

ABSTRACT

We print wax on the paper and turn the composite into a sequentially-controllable, moisture-triggered, rapidly-fabricated, and low-cost shape-changing interface. This technique relies on a sequential control method that harnesses two critical variables: gray levels and water amount. By integrating these variables within a bilayer structure, composed of a paper substrate and wax layer, we produce a diverse wax pattern using a solid inkjet printer. These patterns empower wax paper actuators with rapid control over sequential deformations, harnessing various bending degrees and response times, which helps to facilitate the potential of swift personal actuator customization. Our exploration encompasses the material

mechanism, the sequential control method, fabrication procedures, primitive structures, and evaluations. Additionally, we introduce a user-friendly software tool for design and simulation. Lastly, we demonstrate our approach through applications across four domains: agricultural seeding, interactive toys and art, home decoration, and electrical control.

CCS CONCEPTS

• Human-centered computing → Interactive systems and tools.

KEYWORDS

sequential control method; shape-changing interfaces; programmable material; morphing materials; rapid fabrication.

*Both authors contributed equally to this research.
†Corresponding authors.



This work is licensed under a Creative Commons Attribution International 4.0 License.

ACM Reference Format:

1 INTRODUCTION

Paper stands out as an economical, biodegradable, and extensively utilized natural material in everyday life. Within the field of HCI, paper has found applications in the creation of functional interfaces with the capacity for sensing [11], actuating [8, 34], and energy harvesting [10]. Among many techniques introduced for actuating papers, one of the simplest is to leverage the inherent responsiveness of paper to water. Such a water-triggered response is due to the physics that natural fibers in the paper readily absorb water and swell. Although this actuation phenomenon has been explored by hobbyists and demonstrated in K-12 STEM activities commonly in the form of a blooming flower on water surface [2], it is not until recently that the design and engineering community started to take it as an enabling material for controllable and programmable morphing. In particular, we have seen that paper-plastic bi-layer structure was used to mimic hygromorphic pinecones [28], inkjet-printed water pattern was used to program self-folding paper origami [4], and solid ink printer used to selectively coat wax pattern on paper to design paper robots [30]. In these past works, paper actuator techniques were promoted because of their design versatility and accessibility. However, the controllability of water-triggered actuators is still rather limited, hindering its potential use in more sophisticated interfaces. For example, the sequential control aspects have not been explored. The other well-known physical or fabrication affordances of paper water-triggered actuator, such as the potential for layer-stacking, the integration with kirigami, the fluidic transport and ionic conduction, etc, have not been fully explored in conjunction with its actuation capability. As a result, we believe there is an opportunity to deepen the actuation technique

thus broaden the functional design space of paper actuators, without sacrificing paper's charm of accessibility and rapid fabrication affordances for the maker community [37].

Building on top of existing wax-paper actuator technique [30] that primarily explored simple pattern, non-sequential shape changes with limited paper movements, we devised a collection of techniques to enable sequential control of shape changes in paper actuators, incorporating more intricate patterns, sequential morphing, and increased movements. Furthermore, we have integrated these sequential techniques with diverse structural designs, enhancing their functionality to encompass features such as natural seeding and ionic conduction.

In particular, in order to control the sequential morphing, we explored the functions of wax coating on paper in two ways: 1) By varying gray levels in the printed wax pattern, we can control the morphing sequence under a uniform water spray. In this scenario, the wax coating functions as a controllable water barrier that can hinder water transport. 2) By leveraging the hydrophobicity of wax and printing two parallel lines out of it, we could form a hygromorphic hinge in between the wax line. In this configuration, the geometrical parameters of the hinges, including the hinges thickness and structure characteristics, could control the morphing sequence of the paper actuator.

With the shared objective of achieving multifunctional and controllable paper actuators, we demonstrated how various types of readily available printing paper actuators can exhibit complementary characteristics in terms of morphing responses, water conduction, and actuation reversibility. Furthermore, we explored the potential for integrating electronic components into our paper-based actuators. This entailed harnessing the advantageous qualities of copper tape, including its ease of conductivity, lightweight properties, and user-friendly operation, to merge with wax paper in the creation of circuit switches and other elements. Additionally, although both paper diagnostic microfluidics [18] and paper conductors have been discussed in the past, these techniques have not been leveraged for paper morphing.

The overview of this paper is shown in Figure 2. In this paper, our key contributions, particularly when compared to closely related techniques like paper robotics [30], can be summarized as follows:

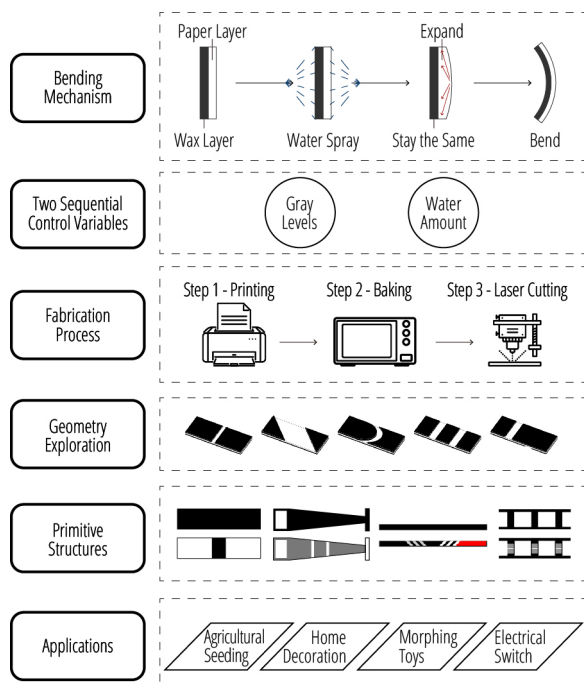


Figure 2: The framework overview of waxpaper actuator.

- (1) Introduction of waxpaper actuator with sequential and conditional morphing method: We integrate the waxpaper actuator into a system that offers sequential and conditional control over shape changes. This includes using gray levels and water amount as independent variables, water spray as the actuation method, and manipulation of bending degree and response speed as dependent variables.
- (2) Development of a set of sequentially controllable morphing structural primitives: We introduce a collection of structures that enable precise sequential control over shape-changing and actuation processes.
- (3) Provision of a design tool for HCI researchers: We offer a user-friendly design tool designed to facilitate digital simulation and fabrication, catering specifically to the needs of researchers in the field of HCI.
- (4) Implementation of applications across diverse scenarios: To demonstrate the practical utility of the waxpaper actuator,

we present applications in four distinct scenarios, including agricultural seeding, interactive toys and art, home environment decoration, and electrical control.

2 RELATED WORKS

2.1 Paper Actuator

Paper actuators have gained widespread use and favor in the HCI field due to their cost-effectiveness, rapid manufacturing, reusability, and biodegradability. Within HCI, paper actuators have found their place by offering versatility and innovative design possibilities, such as interaction design toolkits [26], actuating artifacts [24], soft robotics [30] [31] [5], rapid prototyping [26], and artistic expression [12]. Different techniques to actuate paper have also been developed, such as local heating [34], pneumatic [19] [40] [22], and magnetization [23]. Beyond HCI, paper actuators have been explored extensively as well, including PEDOT:PSS enabled conductive paper actuator [6], natural pollen paper actuator [38] and paper-plastic bi-layers [29]. Among them, wax paper has emerged as a promising candidate due to its distinctive characteristic of bending when exposed to moisture. This characteristic aligns well with the requirements of various HCI applications, including natural seeding, educational tools, home environment decoration, and arts, where moisture-triggered actuation can be advantageous. While paper actuators have primarily relied on external stimuli, such as manual manipulation or forced air, waxpaper actuator introduces a novel, nature-inspired approach to actuation, enabling interaction through the environment. Building on top of literature, we are the first to introduce sequential and conditional programmability into waxpaper actuator.

Furthermore, among the existing paper actuators, some have complex fabrication processes or are easily manufactured but demonstrate limited performance. Notably, Narumi's Inkjet 4D Print [21] stands out by introducing a cost-effective, easily and rapidly fabricated method for shape-changing interfaces, boasting higher printing resolution and faster speed. However, key distinctions exist: 1) our approach uses common paper and hydrophobic wax instead of a polymer sheet and ink. 2) While both projects involve air exposure for activation, Inkjet 4D Print utilizes external heat for bending, whereas our method relies on moisture to increase fiber gap without bending the fibers. 3) Our focus is on a sequential control fabrication method, whereas Inkjet 4D Print emphasizes a self-folding origami tessellation method.

2.2 Wax-Based Actuators

Wax has demonstrated its versatility as a material in various applications, including its use as an actuating material in soft robotics [30], a valve material for microfluidic chips [36], a bonding agent for layers in microfluidic devices [3], an additive to enhance 3D printing materials [32], and a substrate for crafting both 2D [1] and 3D microfluidic channels [27]. The wax printing technique has enabled rapid prototyping with wax actuators, and wax-based fluidic chips have emerged as a potential alternative to traditional PDMS for various bio-testing applications. Despite these promising applications, there are notable gaps in current wax printing research. Firstly, most studies have been limited to using a single black color of wax, neglecting the potential offered by various shades of gray levels

and colors achievable with wax printing. Secondly, the hydrophobic properties of wax-printed bilayer structures, consisting of a wax layer and a paper substrate, are not fully realized until these layers are fused together through baking. Lastly, comprehensive investigations focusing on wax printing as the primary research subject remain relatively limited in number and scope in HCI field. Our research introduces the waxpaper actuator, addressing limitations in wax printing and offering a broader color range and easier actuation method for creative expression in HCI applications.

2.3 Sequential Morphing Interfaces

Sequential control methods for morphing interfaces have been extensively explored in previous research, with dedicated studies or incidental mentions in the literature. For instance, the 4D Mesh utilized PLA shrinking actuators of different sizes and placements, triggered by global heating in water [35]; MilliMorph employed various channel arrangements connecting actuating chambers, triggered by pneumatic actuation [14]; ShrinkCells employed fuses and conductive paths with designated resistance, activated by local heating [20]; EpoMemory utilized materials with varying ratios of crosslinker and epoxy, activated by global heating methods like ovens, heat guns, and hot water [39]. Nevertheless, these control methods often entail the use of complex electrical components or external large-scale devices, which can be time-consuming and costly. Our straightforward process involves printing wax patterns on affordable, everyday papers with varying gray levels, enabling sequential deformations through water spraying. This innovation empowers the achievement of sequential deformations through the controlled application of water, harnessing the unique properties of wax-infused paper for quick and easy actuation.

3 WAXPAPER ACTUATOR SEQUENTIAL CONTROL METHODS

3.1 Material Deformation Mechanism and Variables

3.1.1 Material Deformation Mechanism. Paper absorbs water and expands in proportion to its moisture content due to its porous structure and hydrophilic cellulose fibers. Water molecules that penetrate paper weaken the bond between adjacent cellulose fibers and increase the gaps between the cellulose fibers, enabling hydroexpansion. Due to the hydrophobic wax's ability to clog pores and keep moisture out, the paper does not swell when it is impregnated with it. The hydrophilic region expands while the hydrophobic wax layer does not. Therefore, if a paper is printed with wax on one side, then the side without wax (the hydrophilic side) will absorb water while the wax side (the hydrophobic side) won't, resulting in a bilayer single sheet of paper folding in response to water spray. The disparity in layer expansion causes a localized bending of the paper (Figure 3-b), and altering the influencing variables affects the temporal order in which such difference occurs, allowing for sequential deformation of the wax-printed paper. Figure 3-a shows the structure of waxpaper actuator: a bi-layer structure with a paper substrate and a wax hydrophobic layer. Figure 3-c and d shows the SEM photos of paper printed without and with wax respectively.

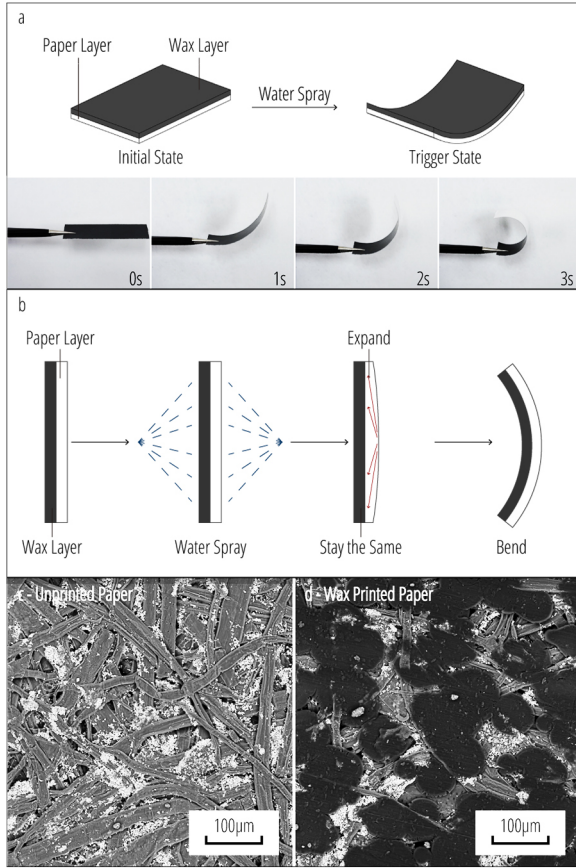


Figure 3: (a) Waxpaper actuator structure and deformation process with water spraying; (b) Section view of bending mechanism; (c) SEM photo of paper without wax; (d) SEM photo of paper with wax.

3.1.2 Variables That Determine the Paper Responding Performance.
 (1) Wax Difference between Paper Sides. To have finer levels of controllability in the bending angle and bending speed, instead of printing wax on a single side, we also introduce a strategy to print wax on both sides yet with different wax density. The degree of bending in our paper actuators is intimately tied to the wax difference between the two sides of the paper. A higher wax difference results in more pronounced and swifter bending. The wax difference reaches its maximum when one side is printed with a full 100% wax coating, while the other side remains wax-free. Conversely, when the wax difference diminishes to zero, no bending actuation occurs upon exposure to water spray. To quantify this wax disparity, we employ the term “Gray Levels”, which range from zero to 100%, reflecting the wax value on each side of the paper.

(2) Water Amount in the Triggering Process. The quantity of water administered during the spraying process directly influences the extent and speed of paper bending. This phenomenon stems from the mechanism of water penetrating the spaces between paper fibers, causing them to expand more significantly and rapidly with greater water input over time. Since one side of the paper actuator is consistently printed with 100% wax, rendering it highly hydrophobic, as a result, water must be sprayed from the side with

a lower gray level. However, it’s crucial to emphasize that these observations pertain specifically to the use of water spray as the triggering method. Dropping or pouring water onto the samples either renders them non-functional or causes irreparable damage.

3.2 Fabrication Process

3.2.1 Set 1: Printing (Figure 4)-a1.

- (1) Place a letter (or A4) size of printing paper substrate in the tray of the inkjet solid wax printer (Xerox Colorqube 8580 or 8570), and print the designed patterns from the computer. In this step, a bi-layer structure with a paper substrate and a wax layer is produced, and the wax layer is right above the paper layer.
- (2) When a double-side printing is needed, repeat the step above and print again.

3.2.2 Set 2: Baking (Figure 4)-a2.

- (1) Bake the printed sample in the oven with the temperature of 300 degree Fahrenheit for 5 seconds. In this step, the wax is gradually melting and getting into the paper layers, which would fill the space between fibers and cover some of the fibers. This step is to make sure that the wax pieces melt into an entity so that there would be no wax pieces produced in the laser cutting process and would keep the operating environment clean.
- (2) We have to note that the waxpaper cannot be overbaked, ideally no more than 5 seconds in the temperature of 300 degree Fahrenheit. If the wax is completely baked into the fibers, the wax difference between two sides of the paper would decrease to 0 (Figure 5), which wouldn’t trigger the bending deformation.

3.2.3 Set 3: Laser Cutting (Figure 4)-a3.

- (1) Finally, laser cut the sample into the designated shapes, and triggers it with water spray from a certain distance. The wax where the laser walks would be totally baked into the fibers because of the high heating temperature.
- (2) In this step, the space between the fibers would swell when absorbing the water and shrink when the water evaporates.

3.3 Sequential Control Method

In this session, we introduce the sequential control method (Figure 6) built upon the waxpaper actuator technology. Within this method, gray levels and water amount assume the roles of independent variables that initiate the triggering process. Gray levels are responsible for modulating the wax-printed pattern on the paper actuator, while water amount governs the distance of the water spray from the target actuator, the primary actuation method employed by the waxpaper actuator. The combined influence of the wax patterns and water spray ultimately determines the degree of bending and the speed of response. To illustrate the practicality of this method, we present four applications across diverse contexts, encompassing agriculture, interactive toys and art, home environment decoration, and electrical control.

Leveraging the insights presented within this method, we gain the capability to tailor and craft waxpaper actuators through the

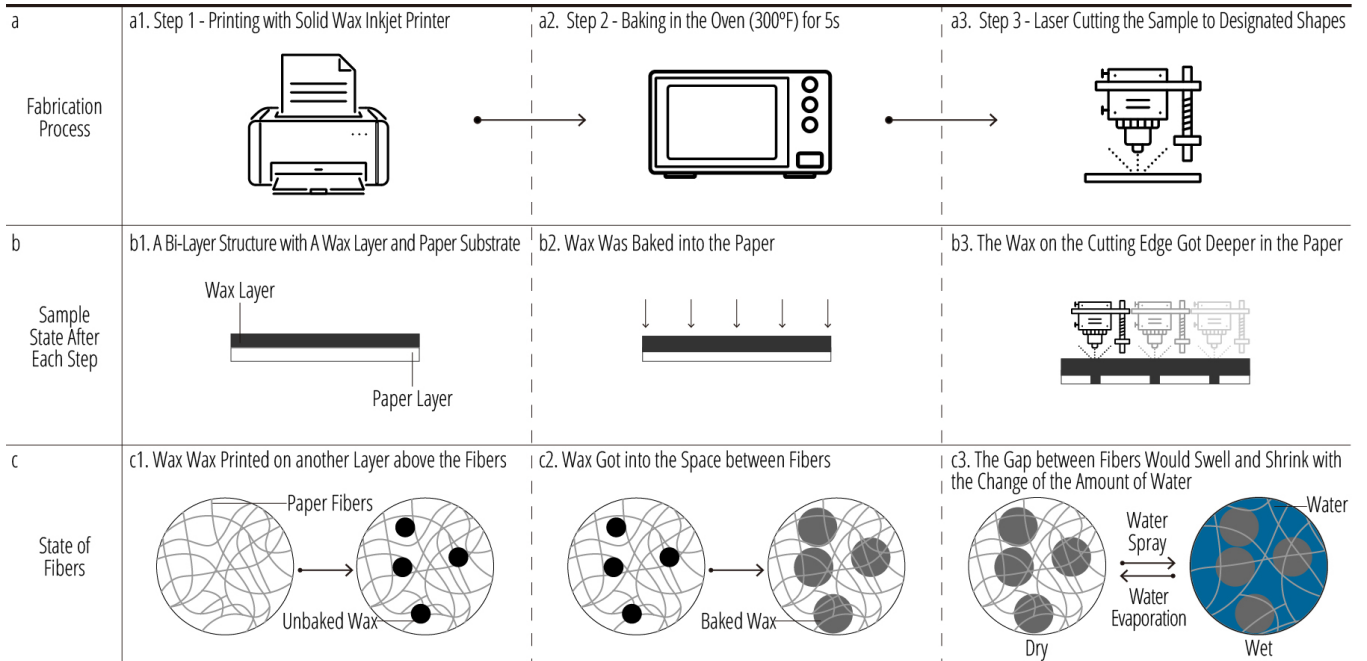


Figure 4: (a) Fabrication process; (b) Section view of sample state after each step; (c) Microview of the state of paper fibers.

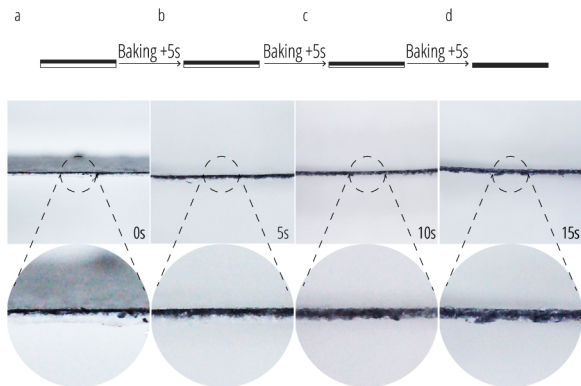


Figure 5: Photos showing sections of paper with different baking times. (a) Unbaked wax paper. (b) Wax paper with a single layer baked for 5 seconds. (c) Wax paper with a single layer baked for 10 seconds. (d) Wax paper with a single layer baked for 15 seconds.

design of precisely printed patterns with varying gray levels. Additionally, we can exert control over the water amount by adjusting the distance of the water spray, thereby achieving a large space in the design and utility of waxpaper actuators. This approach enables us to delve deeper into the possibilities of waxpaper actuator applications, unveiling intriguing prospects within this design realm.

3.4 Geometry Exploration

As we explore various geometric forms for waxpaper actuators, it's essential to highlight that all seven geometry samples follow a

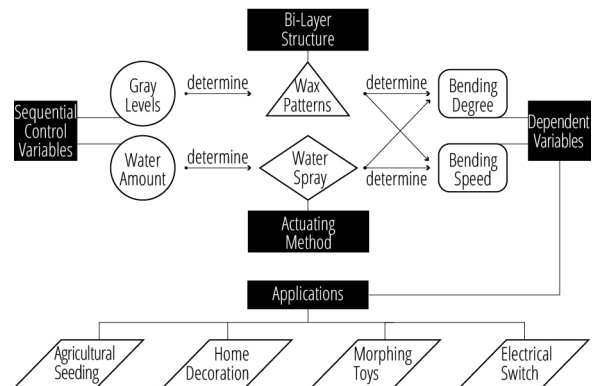


Figure 6: Overview of the sequential control method for wax-paper actuator.

shared design approach. Each of them is printed with a 100% gray level wax layer on one side and features designated patterns on the other side. The only exception is Figure 7-c2, where the same pattern is printed on both sides. This unique design enables the unprinted white region to act as the actuator when exposed to water spray. These geometries are further categorized into three distinct groups:

- (1) Perpendicular Hinges with Different Thicknesses (Figure 7-a): Within this category, Figure 7-a1, a2, and a3 showcase perpendicular hinges of varying thicknesses, measuring 3mm, 6mm, and 20mm, respectively. These hinges exhibit impressive bending capabilities, achieving angles of up to 60 degrees, 90 degrees, and 180 degrees after just one water spray.

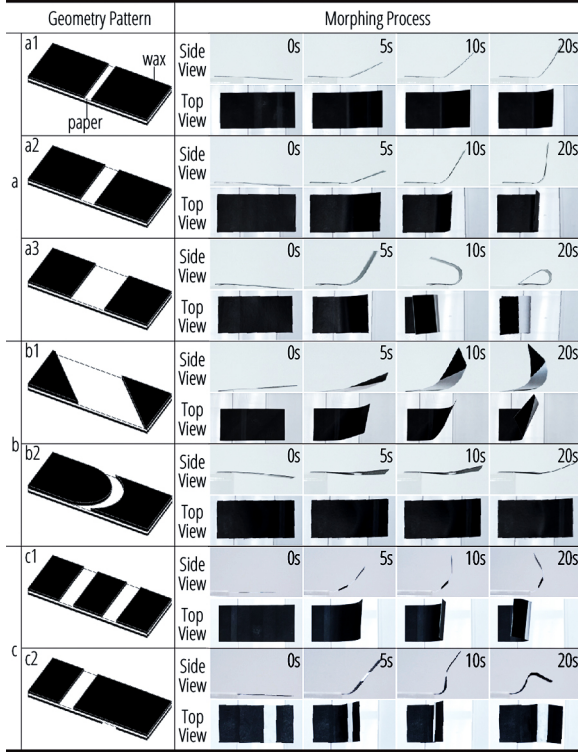


Figure 7: (a) Perpendicular Hinges with Different Thicknesses; (b) Angled Hinges; (c) Multi-Segment Hinges.

- (2) Angled Hinges (Figure 7-b): Figure 7-b1 and b2 introduce angled hinges featuring distinct patterns. The former employs slanted lines at a 45-degree angle, while the latter adopts an arc line pattern. When triggered by water spray, these hinges not only bend in the designated directions but also form specific shapes, adding an element of dynamic design to their functionality.
- (3) Multi-Segment Hinges (Figure 7-c): This category encompasses Figure 7-c1 and c2, which present multi-segment hinges with unique characteristics. Figure 7-c1 boasts two hinges on one side, culminating in a final "U" shape upon actuation. In contrast, Figure 7-c2 features a single hinge on each side, resulting in a distinctive "S" shape transformation after activation.

These explorations across three distinct geometric types enhance the diversity of pattern forms and their corresponding actuated shapes. This diversification lays a strong foundation for the development of primitive structures and potential applications, further expanding the horizons of our waxpaper actuator technology.

3.5 Development of Primitive Structures

Through our exploration of two variables and geometric shapes, we've created four fundamental waxpaper actuator structures. Each of these structures offers the potential for sequential actuation, enabling diverse forms of movement, ranging from flat sheet transformations to volumetric changes.

3.5.1 Strip Primitive with Perpendicular Hinges. This primitive shows how regions with different gray levels deform in different velocities, leading to sequential shape change of a body. As shown in Figure 8-a, we print wax of 100% gray level shape on the front side of the paper. And on the back side of the paper, we print wax of 100% gray level with two wide 40% gray level strips that overlap with the zero strips. To trigger the deformation, the sample is sprayed with water from the back side. The white regions with zero gray level will absorb the water the fastest and start to bend to form sharp folds within 30s (Figure 8-a.II). In about 60s, the white regions are fully soaked and the sharp folds will disappear (Figure 8-a.III). Subsequently, the gray regions with 40% gray level on the back side of the paper will start to absorb water and bend. Since these regions are wider than the white regions, the bending is more curved (Figure 8-a.IV).

3.5.2 Strip Primitive with Multi-Segment Angled Hinges. This primitive shows how to assemble a body into a sequentially shape-changing structure with multi-segment angled hinges. As shown in Figure 8-b, on the front side of printing paper, we print 3 lines of 20% gray level 135 degree above horizontal line on left side and 3 lines of 0% gray level 45 degree above horizontal line on right side. On the back side of tracing paper, 100% gray level is printed. To trigger the deformation, the sample is sprayed with water from the front side. The 0% gray level region on the right would react the faster and immediately bend within 30s (Figure 8-b.II). The 20% gray level region on the left would react in the next 30s (Figure 8-b.III). In 90s, the printed tracing paper would finish assembling, with right end under left end due to sequential bending (Figure 8-b.IV). Note that the right end is printed with red wax for visual identification purposes.

3.5.3 Self-Locking Structure. As shown in Figure 8-d, we wax the front of the pattern with 100% gray scale. On the back, except for the hinge (10% gray level) and the tail structure (0 gray level) at the right end, wax is printed with 100% gray level in other areas. The lock mechanism is activated by spraying water from the bottom side. Lower gray levels result in faster reaction speeds and quicker completion of the reaction. As a result, the thin strip with a 0% gray level curls into a small ball and unlocks before the overall folding process, effectively securing the entire structure prior to bending and flattening. (Figure 8-d.I to IV).

3.5.4 Volume Primitive with Horizontal Hinges. This primitive shows the use of the first primitive assembled in the form of volume. As shown in Figure 8-c, we print 100% gray level of wax on the outside of the paper. And on the back side of the paper, we print wax of 100% gray level with two wide 40% gray level strips that overlap with the 0% strips on the inside. To initiate the deformation, the sample is sprayed with water from the inside. Notably, the zero gray level region in the middle exhibits rapid reactivity, bending within a mere 30 seconds (as depicted in Figure 8-c.II). Conversely, the surrounding 40% gray level region near the zero gray level area initially responds by forming a sharp shape within the subsequent 60 seconds (as shown in Figure 8-c.III). Subsequently, over a span of 120 seconds, this region gradually transitions into a more curved shape as increased moisture permeates the paper layer through the wax (illustrated in Figure 8-c.IV).

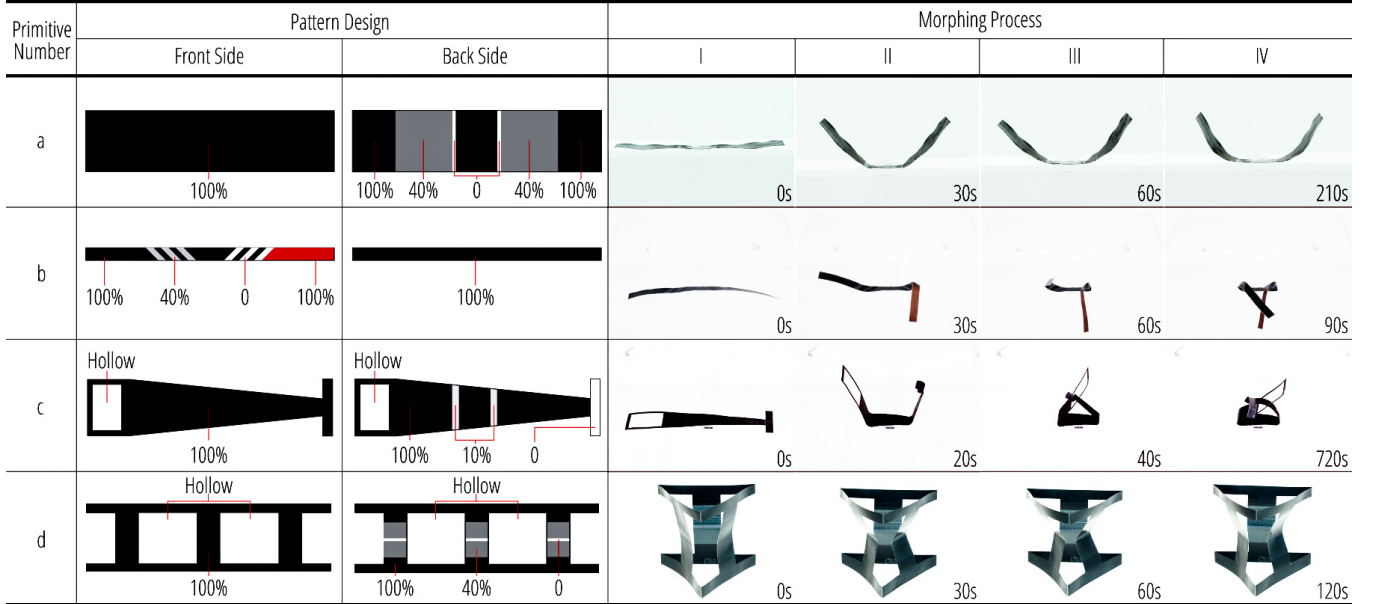


Figure 8: (a) to (d): pattern design of each primitive structure with the percentage values of wax; (I) to (IV): each triggered primitive with time tag.

4 WAXPAPER ACTUATOR EVALUATION

In this session, we conducted an evaluation of two sequential control variables: gray levels and water amount, alongside an evaluation of the reusability. We controlled the size of the test sample, and described the experimental setup and triggering method in detail, with curvature as the test unit. All the experiments detailed below were conducted under specific conditions: a temperature of 22 degrees Celsius and a humidity level of 50%.

Specifically, the evaluation session aimed to examine the interplay between two parameters (gray levels and water amount) and their corresponding responses (bending speed and bending curvature). Furthermore, the data from the evaluation session would help to build the design tool for a more accurate simulation and customization.

Differences exist between our experiments and previous works: 1) We investigated the influence of gray levels as a variable that could affect sequential morphing, an aspect not explored in the previous work, which does not delve into gray levels and their impact on the morphing process. 2) Both our study and the previous work discuss the influence of water amount on morphing behavior. However, while we conducted this by spraying water at various distances to the sample and explored how water amount affects bending curvature and speed, the previous work focuses on using different water amounts to achieve various shape changes. 3) The previous study assessed bending curvature by spraying water on paper multiple times, but it did not assert or develop an evaluation of reusability. In contrast, we explored the reusability of the waxpaper actuator by spraying the same water amount on it at the same distance until the waxpaper actuator sample ceased to function.

4.1 Gray Levels for Wax Difference

The objective of this session is to investigate the impact of gray levels on bending behavior, encompassing both bending curvature and speed. Additionally, it aims to generate data for the design tool, facilitating the simulation of more accurate curvature at the appropriate moment.

We test the relationship between wax difference and its bending curvature as well as how much time it takes. We control the size of wax paper to be 20mm by 60mm and provide excess evenly sprayed water from a distance of 100mm. In the printing process, we print one side of the paper at the wax level of 100%, and gradually increase the wax level on the other side from 10% to 100% (Figure 9). Gray levels would be the independent variable (Figure 10-c), and bending curvature would be the dependent variable. Note that "responding time" refers to the duration from initiation (as depicted in Figure 10-b1) to reaching maximum response (Figure 10-b3).

Samples cease to respond to moisture once the gray levels on the front side reach 60%, consequently, our chart (Figure 10-a) focuses on showcasing the gray levels from 10% to 50%. The performance of our tested samples consistently reveals a clear correlation: a rise in wax difference correlates with heightened bending curvature, a reduced time to reach maximum curvature, and a prolonged duration of deformation. As evident in Figure 10-e and Figure 10-f, higher gray levels on double-sided printed wax paper result in reduced bending curvature and slower actuation of the waxpaper.

4.2 Water Amount

The goal of this session is to comprehend the impact of water amount on the paper's bending behavior, encompassing both bending curvature and speed. Additionally, it aims to produce data for

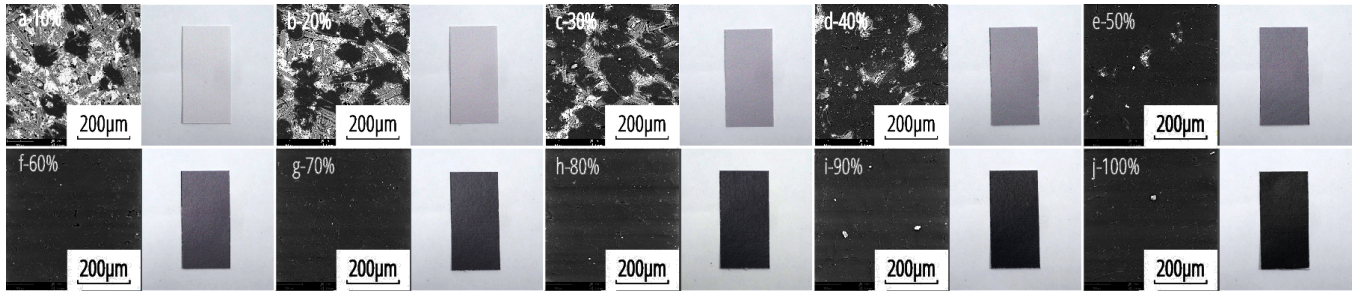


Figure 9: SEM photos and real photos of paper with wax gray levels from 10% to 100%.

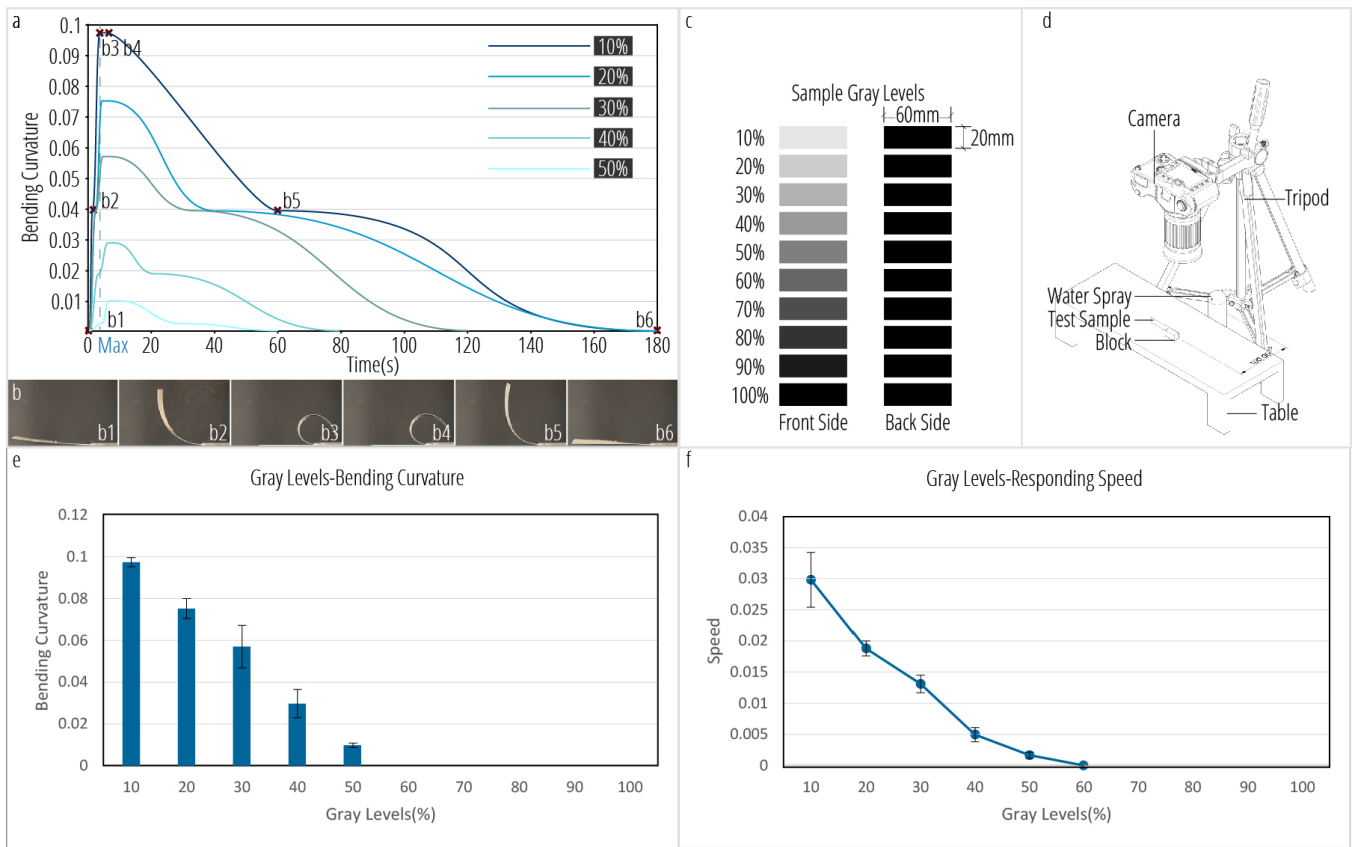


Figure 10: (a) Relationship between bending curvature and responding time for waxpaper samples with front side gray levels from 10% to 50% with one time spray; (b) Morphing process for waxpaper samples with front gray level of 10%. Sample size for each curve: $n = 1$. (c) Testing samples in different gray levels; (d) Experiment setups; (e) Relationship between gray levels and bending curvature. Sample size for each gray level: $n = 3$; (f) Relationship between gray levels and responding speed. Sample size for each gray level: $n = 3$.

the design tool, streamlining the simulation of more accurate curvature at the opportune moment. In this session, we embark on an exploration of the relationship between water amount and its impact on bending curvature and response time in waxpaper actuators. Within this study, we have standardized the size of our samples (20 mm by 60 mm)(Figure 11), and consistent gray levels. The samples are positioned at varying distances from the water spray source,

set at 50mm, 100mm, 150mm, 200mm, 250mm, 300mm, and 350mm (Figure 11-b). In addition, we employed a method by weighing the samples both before and after triggering the water spray, which enables us to quantify the amount of water absorbed by the samples at each corresponding distance (as illustrated in Figure 11-c). The outcomes of our testing consistently reveal a well-defined correlation, as depicted in Figure 11-d and Figure 11-e: an increase in

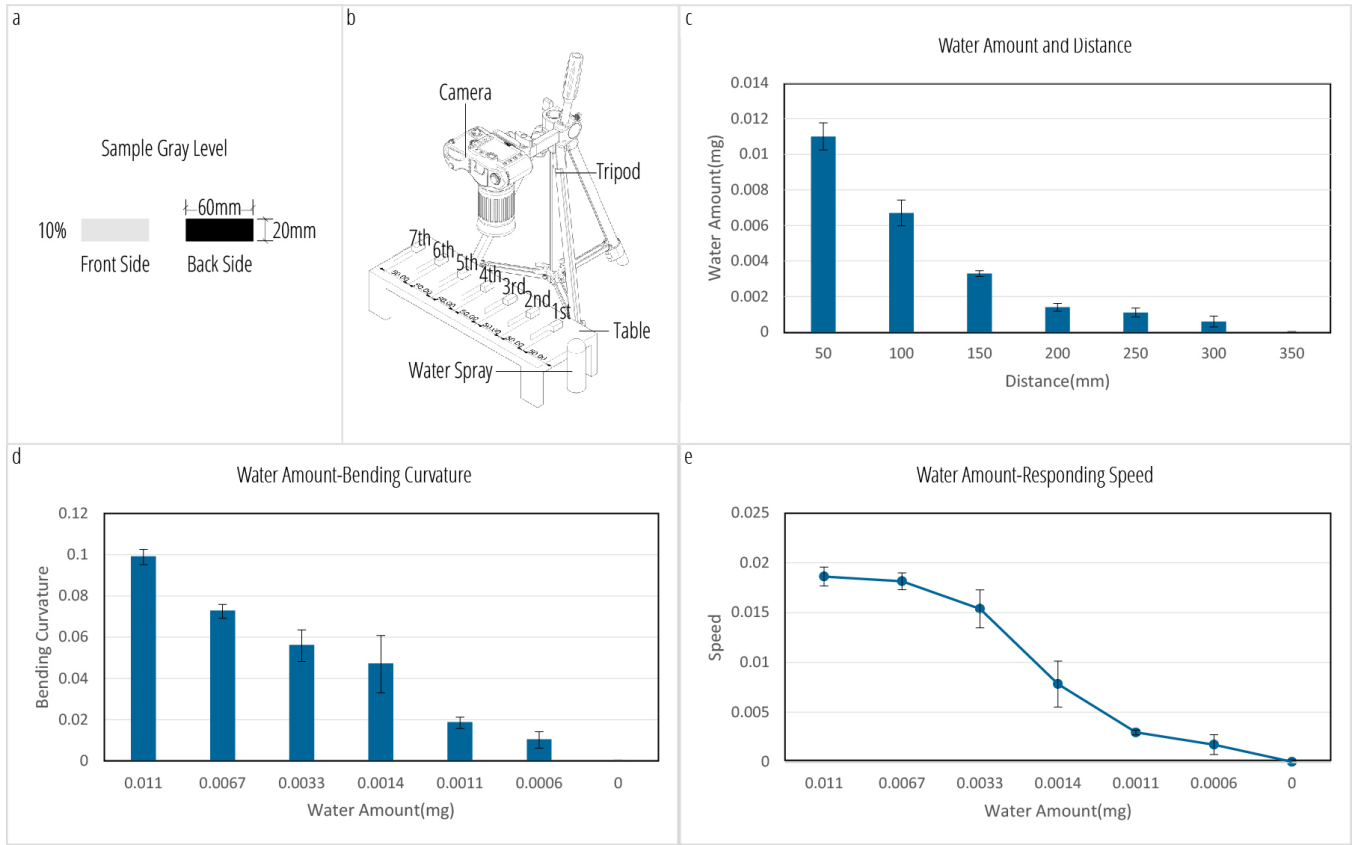


Figure 11: (a) Testing sample; (b) Experiment setups; (c) Relationship between triggering distance and water amount. Sample size for each distance: $n = 3$; (d) Relationship between water amount and bending curvature. Sample size for each water amount $n = 3$; (e) Relationship between water amount and responding speed. Sample size for each water amount: $n = 3$.

the volume of water applied to the same sample is directly linked to a heightened bending curvature and a reduced time required to reach maximum curvature.

4.3 Resuability

In this session, our aim is to assess the number of times the wax paper actuator can be reused under typical ambient conditions. The setup for testing the reusability of the waxpaper actuator closely mirrors that of the gray levels evaluation (Figure 12-b). Throughout the experiment, the testing sample remains stationary in the same position, consistently triggered by a one-second water spray from a distance of 100mm with each press. We record two critical data points: the maximum bending angle when the actuator is wet and the bending angle when all water has evaporated. This process is repeated iteratively until the bending angle upon water evaporation becomes significant, rendering the hinge area, which serves as the actuator, unable to receive moisture from the water spray. As illustrated in Figure 12-a, the 20 mm by 60 mm waxpaper actuator, equipped with a 20 mm hinge, exhibits reusability, with the capacity for up to seven uses (Figure 12-c). After each test cycle, the maximum bending angle when wet gradually diminishes, while the bending angle upon complete water evaporation progressively

increases, ultimately reaching 90 degrees. This data showcases the practical lifespan and endurance of the waxpaper actuator in a reusable context.

5 DESIGN AND SIMULATION TOOL

In this session, we introduce a computational simulation tool designed to replicate the bending behavior of wax paper actuators on basic shapes, along with its geometrical mechanism and walk-through process.

5.1 Geometrical Mechanism of Waxpaper Actuator

This tool is designed to replicate the sequential morphing process of the double-sided printed wax paper actuator triggered by a single water spray from a 100mm distance in the time period from 0 seconds to the time it reaches the maximum curvature value. Consequently, the tool exclusively incorporates data from experiments involving various gray levels.

The tool consists of three primary sessions: pattern selection, assignment of gray levels to each part of the pattern, and finally, simulation to observe the sequential morphing of different sections.

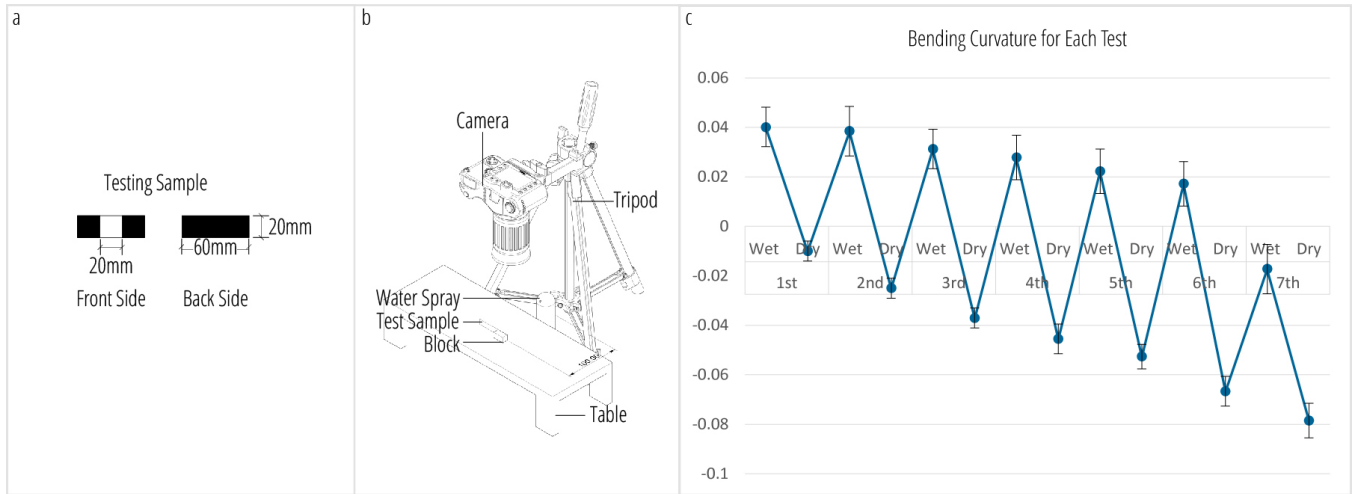


Figure 12: (a) Testing sample; (b) Experiment setups; (c) Bending angle in each triggering time. Sample size for each test: $n = 3$.

In the gray level experiment, we examined the relationship between gray level and curvature, and the correlation between gray level and speed. The wax paper exhibits distinct bending curvature at specific times (Figure 13). Therefore, we computed for each gray level and found that the relationship between time and curvature conforms to the following functional equation:

$$b = y * t$$

where y is the bending constant, b is the bending curvature, t is the reaction time (in seconds) and the domain of t is the time period from 0 seconds to the time it reaches the maximum curvature value (0 to T_{max}). The relationship between gray level and bending constant is governed by the following functional equation:

$$y = 0.0484e^{-0.0503g}$$

where g is the gray level (from 10% to 50%). It's important to note that this relationship is contingent on the specific materials and methods used in our experiments. Variations such as different brands of paper could necessitate adjustments to the constant in the equation. Such changes might arise from differences in thermal properties, structural integrity, or the paper's absorbency, which could all influence the actuator's response to moisture.

Subsequently, we input this functional relationship into the curvature control module in Grasshopper. Ultimately, after users complete the pattern and gray level selections, they can observe the sequential bending process of the chosen pattern by adjusting the time slider.

5.2 Walk-through Process

Utilizing Rhino 6 as the foundational design environment and harnessing the power of Grasshopper and Human UI as intermediate interfaces, this software integrates into the design process of printed paper actuators.

Step 1: Select your desired pattern (Figure 14-step 1). You have the option to either create your own pattern or choose patterns from the pattern library, which include geometric explorations, primitive structures, and various applications.

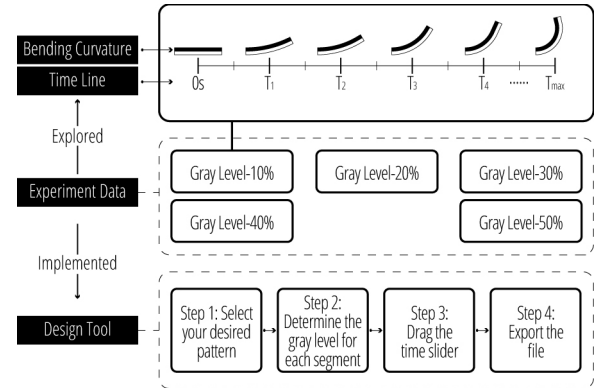


Figure 13: Mechanism of the design tool.

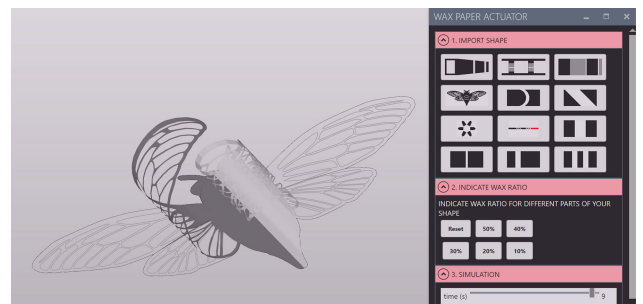


Figure 14: The interface of design tool.

Step 2: Determine the gray level for each segment of the pattern, ranging from 10% to 50% (Figure 14-step 2). Given that the experiment has demonstrated the lack of moisture response in the double-sided printed wax paper actuator when the gray level exceeds 60%, we limit the gray levels to the range of 10% to 50%.



Figure 15: (a) Fabrication process - a1. Laser cut the designated waxpaper patterns, a2. Fold the flat pattern into the volume seed container, a3. Add the soil, a4. Lock the device, a5. Flip over the volume, a6. put seeds on it; (b) Seeds releasing process: seeds and soil fall one after another in sequences with time tags.

Step 3: Drag the time slider and check the morphing process (Figure 14-step 3). As time progresses, regions with different gray levels will sequentially undergo bending.

Step 4. Export line file. Users can export the line file in PDF format from Rhino 6 for laser cutting or 2D printing.

6 APPLICATION

6.1 Sequential Seed Dispenser

The first application showcases the sequential seed dispenser, highlighting its utility in the field of agriculture by demonstrating automatic seeding triggered by natural moisture, such as rain. This device, depicted in Figure 15-a, incorporates two distinct actuators: the tail actuator, designed with a tail structure to support the weight of soil, and the seed actuator, responsible for holding the seeds. While both actuators feature a 100% wax coating on their

back sides, their front sides differ in wax application. The tail actuator is printed with a 30% gray level, whereas the seed actuator remains unwaxed. This deliberate choice offsets the gravitational influence of soil weight on the tail, preventing premature actuation. Without the higher gray level wax on the tail actuator to delay its response time, simultaneous exposure to moisture would lead to soil dropping to the ground first due to its greater weight, leaving the seeds uncovered and unable to germinate. Figure 15-b illustrates the seeding process in detail. Initially, the seed dispenser is filled with soil and seeds, with the latter placed in their designated region at the top. Subsequently, water is sprayed from the top using multiple presses to simulate natural rain conditions. Both actuators begin to bend in response to the moisture. Thanks to the seed actuator's relatively lighter gray level, the seeds are the first to descend to the ground, followed by the soil, which covers the seeds.

This application underscores the potential of the waxpaper actuator in agriculture. By enabling automatic seeding triggered by

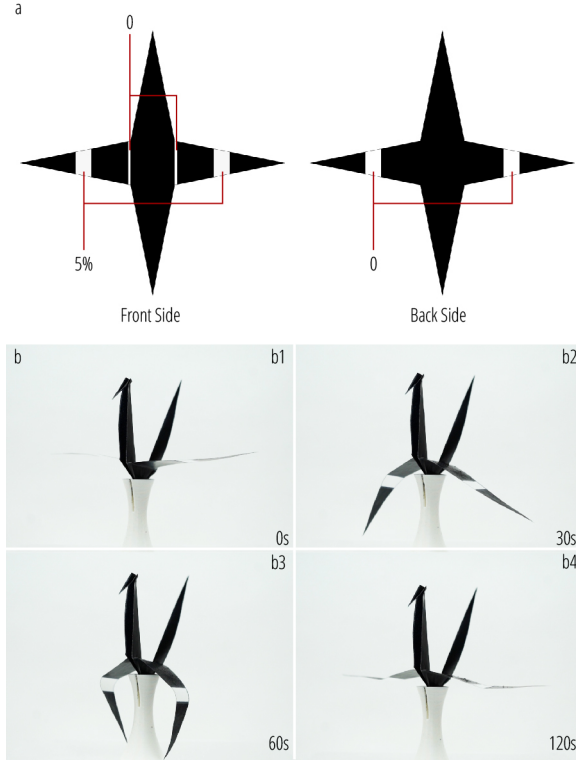


Figure 16: (a) Printing illustration of crane morphing toy (percentage values indicate gray levels of wax); (b) Crane sequentially folding wings with time tag.

natural moisture with a low-cost, rapid-fabricated and assembled, and biodegradable approach, it offers a solution for agricultural production. This not only enhances seeding efficiency but also has the potential to reduce resource wastage, fostering the development of sustainable agricultural practices.

6.2 Morphing Toys

6.2.1 Crane. The first morphing toy is the Crane. The paper used for making the crane is coated with wax on both sides. As shown in Figure 16, on the front side of the paper, we left two lines at the base of the crane's wings without wax printed (0 percent) to facilitate bending after spraying with water. On both sides of the paper, towards the middle of the crane's wings, a larger blank area was left. The front side was coated with 5% wax, while the back side had 0% wax coating. This application demonstrates the sequential triggering of different deformation responses of the paper after water spraying, depending on the presence or absence of wax. When water is sprayed from above, the smaller contact area at the base of the wings causes the paper to bend downward first. Then, the paper towards the middle of the wings bends inward. After a reaction time, the base of the paper starts to recover upwards, and the middle of the wings returns to their original position. Once the crane's shape has been restored, we can repeat the experiment after the water is dry. Note that this process is repeatable when water is provided with a limited amount when triggering, and completely evaporated after use. This example demonstrates how our sequential control

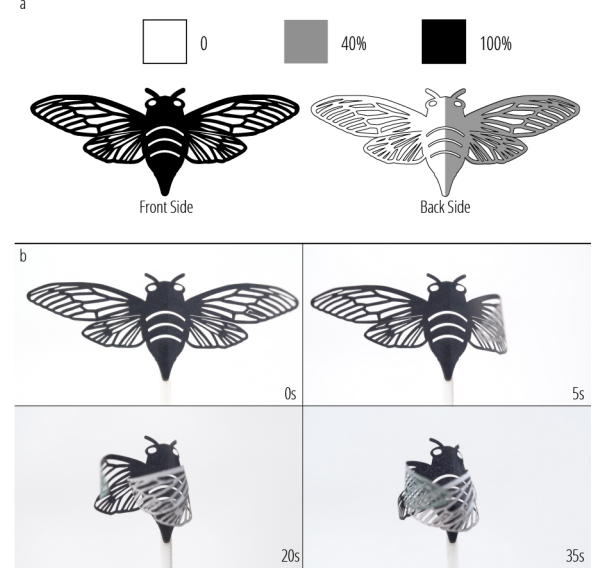


Figure 17: (a) Printing illustration of cicada morphing toy (percentage values indicate gray levels of wax); (b) Cicada sequentially folding wings with time tag.

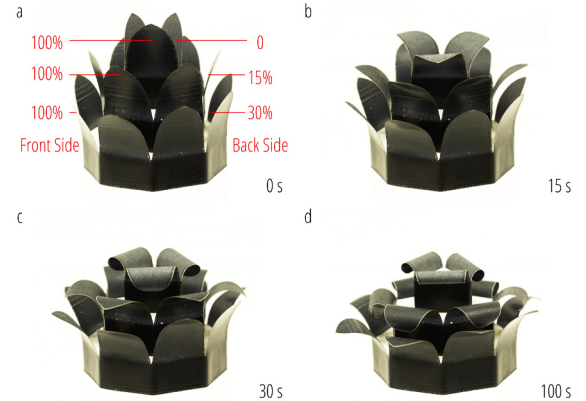


Figure 18: Layered sequential blooming of a rose flower with wax levels and time tag.

technique can be easily integrated with origami. Therefore, we can envision a series of origami artifacts that can be designed with this method.

6.2.2 Cicada. The second morphing toy is the Cicada, which utilizes similar characteristics. As shown in Figure 17, the front side of the Cicada is coated with 100% wax, while the back side is divided into two sections along the central axis. The left side is sprayed with 40% wax, while the right side has no wax coating at all. After spraying water on the back side, the right side will respond more quickly than the left side, causing the right side to bend before the left side.

6.2.3 Morphing Flowers. The third morphing toy - Morphing Flowers - demonstrates the sequential blooming of the petals when water



Figure 19: (a) Fabrication process - origami to fold into the shade in different depth and distance; (b) Different regions in the lampshade bend in sequences with time tags.

is introduced by spraying. As shown in Figure 18, the flower is made up of 3 layers of wax printed paper with 100% gray level wax printed on the external side, and 0, 15%, and 30% gray level wax on the internal side from the top to the bottom layers respectively. When water is sprayed from 10s above the flower with 3 presses (1 second for each press), the petals will bloom sequentially from the top to bottom.

6.3 Responsive Lampshade

The third application combines with origami, utilizing varying water amounts in different distances to control the triggering. As shown in Figure 19-a, one side of the origami is coated with 100% wax (to match the color of the light, we printed it with orange-colored wax), while the other side remains untreated. The folding of the structure results in different distances from the trigger point, leading to different water amounts and, consequently, sequential deformations. Rectangles of varying heights are cut from a letter-sized sheet of paper. When folded, they create arches of different depths. As you move further into the arch, the depth increases, and the distance from the trigger point also varies. We have printed three types of wax paper, with the back of each being 100% wax. The first has 10% wax sprayed on the front, the second has 30%, and the third has 50%. When these are inserted between the arches and water is sprayed on the front side, it results in a layer bending first, then revealing the second layer, which bends next, followed by the appearance of the third layer. Eventually, all layers bend, revealing the entire arch (Figure 19-b).

6.4 Electrical Exploration - Introducing Waxpaper Actuator as A Switch

In this session, we developed two switches made with waxpaper actuators. By changing the gray levels of the designated area on the paper switches and spraying distances, we can realize the sequential control of how long it takes for the switches to be turned on or

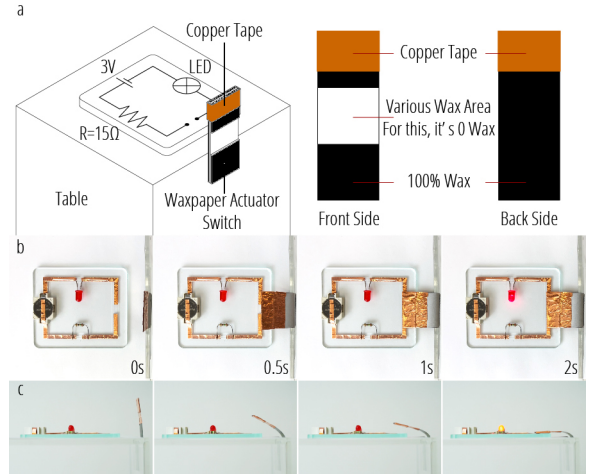


Figure 20: (a) Setups and details of the switch; (b) Top view of the waxpaper morphing switch; (c) Side view of the waxpaper morphing switch.

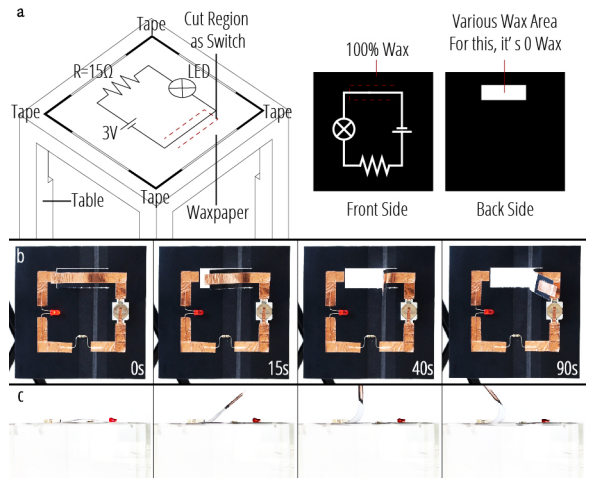


Figure 21: (a) Setups and details of the switch; (b) Top view of the waxpaper morphing switch; (c) Side view of the waxpaper morphing switch.

off within a certain time range. Looking forward, combining such switches may lead to more complex mechanical computation for interface design [7, 16].

6.4.1 The “On” Switch. The following structure (Figure 20) combines wax paper and a circuit to mimic the bending characteristics of the paper when exposed to water, functioning like a circuit switch. We vertically fix a piece of paper on a perpendicular table corner, leaving a small strip of white paper at the upper end of the paper that touches the table corner. The rest of the paper is coated with 100% wax, simulating the area that makes contact with the circuit. Copper is attached to this area. When water is sprayed onto the front side of the actuator switch, a portion of the paper bends, allowing the copper to connect the circuit, causing a small light to turn on. It’s important to note that this device has a limited

lifespan, as after 60 seconds, the paper returns to its initial position, disrupting the circuit. Moreover, the added weight at the upper end of the paper, owing to the attached copper, contributes to the device being single-use. In the future, a potential improvement could involve printing wax on conductive paper to retain both conductivity and the lightweight properties of the paper actuator, enhancing its sustainability and reusability.

6.4.2 The "Off" Switch. In addition to the "On" switch, we have introduced an "Off" switch that employs gravity for reusability (Figure 21). In this application, when water is not present, the circuit remains consistently connected. However, upon spraying water, the paper upwardly bends, interrupting the circuit. During the subsequent recovery phase, gravity plays a pivotal role as the wax paper with copper affixed gradually descends back onto the circuit plane, restoring the connection. This design allows for repetitive use of the switch, offering enhanced sustainability and functionality.

7 DISCUSSION, LIMITATION AND FUTURE WORK

7.1 Versatility and Accessibility

Versatility: by introducing a sequential control method, this paper explores the multifunctionality of paper-based actuators. While the current content provides a preliminary understanding of the versatility of paper-based actuators, future research can further showcase their practical potential in various fields such as agricultural automation, interactive educational toys, artistic installations, home decor, or precision electronic control systems by discussing specific application scenarios in greater detail. Additionally, the capabilities of the waxpaper actuator can potentially be further expanded by integrating liquid metal for circuitry [15, 33], colorimetric chemicals for detection [9], and other enhancements.

Accessibility: this study introduces a user-friendly, responsive, and cost-effective paper-based actuator, aiming to enhance its accessibility. Future research can provide concrete examples to illustrate how this paper-based actuator can be more easily adopted by a broader audience in different fields. For instance, detailing the simplified manufacturing processes required for this actuator and explaining how it can be produced under low-cost conditions will further underscore its contribution to accessibility. This discussion will contribute to a more comprehensive examination of the practical impact of paper-based actuators on broad uses.

7.2 Potential Impact of Ambient Temperature and Moisture Levels

Because our driver is intended for everyday use, our temperature and humidity testing range is based on the typical temperature and humidity levels in human daily life. However, following a series of rapid tests, we observed no significant differences in the behavior of the morphing wax paper actuator across a range of temperatures (0 degrees Celsius to 45 degrees Celsius) or various moisture levels (50% to 80%).

7.3 Scalability and Force-Strength Limitations

The scalability of the wax actuator faces a primary constraint imposed by the size limitation of the printing sheet used as a substrate,

which is restricted to 8.5 inches by 11 inches in the inkjet solid wax printer. Consequently, all demonstrations and applications discussed earlier are executed at a letter-size scale, posing limitations on the efficacy of the wax actuator for larger-scale applications. To address this issue, a potential solution involves assembling letter-size papers using a specific method (such as gluing or stitching) to construct larger-scale items tailored to our purposes.

In addition to scalability concerns, another inherent limitation of waxpaper actuators pertains to their restricted force and strength capabilities. While excelling in providing controlled sequential movement, these actuators face challenges when it comes to exerting force or withstanding heavy loads. This limitation becomes particularly significant in applications requiring substantial mechanical power or resistance to external forces. As part of future work in this area, exploring material enhancements or hybrid designs may offer avenues to augment the force and strength attributes of waxpaper actuators, thereby expanding their utility across a broader spectrum of applications.

7.4 Instability and Inaccuracy

Waxpaper actuators, despite their remarkable capabilities, may exhibit certain levels of instability and inaccuracy in specific scenarios. Factors such as variations in environmental conditions, humidity levels, or wax distribution can introduce unpredictability into their actuation behavior. Moreover, achieving precise and repeatable movements can be challenging, particularly in applications demanding high accuracy. Addressing these issues may necessitate advanced control algorithms, improved manufacturing processes, and thorough testing and calibration procedures. The pursuit of greater stability and accuracy remains an important area for future research, with the potential to unlock new applications and expand the usability of waxpaper actuators.

7.5 Sustainability

Sustainability is an increasingly important topic in morphing interfaces [13, 17, 25]. Wax production frequently involves the extraction of petroleum or other nonrenewable fossil fuels, which contributes to greenhouse gas emissions, so its negative impact on the environment must be taken into account when making consumption and disposal decisions. Compared to petroleum-based wax, beeswax and soy wax are renewable, biodegradable, and produce fewer hazardous pollutants when heated. Therefore, they have the potential to replace the present printing wax material.

In addition, the paper portion of wax-printed paper, however, is recyclable, reusable, and biodegradable. We believe that wax-printed paper shape-changing interfaces are sustainable and can supplement or replace conventional interfaces or electrical devices in some cases, such as interior humidity detectors and sequential seeding where paper does not require recycling, etc.

7.6 Limited Simulation in the Design Tool

One notable limitation of this design tool is its potential difficulty in accurately simulating highly complex shapes and intricate geometries due to its emphasis on simplicity. To address this limitation in the future, we aim to enhance the tool's capabilities by incorporating more advanced simulation features and algorithms, allowing

for the accurate modeling of complex geometries and a wider range of materials.

8 CONCLUSION

In conclusion, our work introduces an approach utilizing moisture-triggered waxpaper actuators for sequentially-controllable shape transformations. By harnessing two pivotal variables, gray levels and water amount, we have empowered these actuators to swiftly manipulate sequential deformations, including diverse bending degrees and responding times. Our study delves into the material mechanisms, sequential control methods, fabrication processes, fundamental structures, and comprehensive evaluations. Additionally, we introduce a user-friendly design and simulation software tool to facilitate experimentation and simulation. Finally, we showcase the practicality of our approach through versatile applications encompassing agricultural seeding, interactive toys and art, home decoration, and electrical control. We believe that our waxpaper actuator, coupled with the sequential control method, will benefit the HCI community through its low-cost and simple fabrication process, as well as facilitating rapid personal actuator customization.

ACKNOWLEDGMENTS

The authors acknowledge the support from the National Science Foundation Career Grant IIS-2047912 (LY). We express our gratitude to Dr. Dinesh K. Patel from the Morphing Matter Lab at Carnegie Mellon University for offering valuable feedback on wax-related printers. Furthermore, we express our gratitude to Michael Vinciguerra, Humphrey Yang, and Lea Albaugh from Carnegie Mellon University, as well as Tianyu Ma from Tsinghua University, for their valuable ideas and feedback to the development of the paper.

REFERENCES

- Emanuel Carrilho, Andres W. Martinez, and George M. Whitesides. 2009. Understanding Wax Printing: A Simple Micropatterning Process for Paper-Based Microfluidics. *Analytical Chemistry* 81, 16 (2009), 7091–7095. <https://doi.org/10.1021/ac901071p> arXiv:<https://doi.org/10.1021/ac901071p> PMID: 2037388.
- Crystal. 2022. Magic blooming flower kids' stem activity. <https://thestemlaboratory.com/magic-blooming-flower/>
- Xiuhong Gong, Xin Yi, Kang Xiao, Shunbo Li, Rimantas Kodzius, Jianhua Qin, and Weijia Wen. 2010. Wax-bonding 3D microfluidic chips. *Lab Chip* 10 (2010), 2622–2627. Issue 19. <https://doi.org/10.1039/C004744A>
- Christophe Guberan. 2012. Studio Guberan. <http://www.christopheguberan.ch/hydro-fold/>
- Mahiar M. Hamed, Victoria E. Campbell, Philipp Rothmund, Fırat Güder, Dionysios C. Christodouleas, Jean-Francis Bloch, and George M. Whitesides. 2016. Electrically Activated Paper Actuators. *Advanced Functional Materials* 26, 15 (2016), 2446–2453. <https://doi.org/10.1002/adfm.201505123> arXiv:<https://onlinelibrary.wiley.com/doi/pdf/10.1002/adfm.201505123>
- Yusuke Hara and Yoshihori Yamaguchi. 2014. Development of a Paper Actuator with PEDOT:PSS Thin-Films as An Electrode. *Actuators* 3, 4 (2014), 285–292. <https://doi.org/10.3390/act3040285>
- Alexandra Ion, Ludwig Wall, Robert Kovacs, and Patrick Baudisch. 2017. Digital mechanical metamaterials. In *Proceedings of the 2017 CHI Conference on Human Factors in Computing Systems* (Denver, Colorado, USA) (CHI '17). Association for Computing Machinery, New York, NY, USA, 977–988.
- Harshika Jain, Kexin Lu, and Lining Yao. 2021. Hydrogel-Based DIY Underwater Morphing Artifacts: A Morphing and Fabrication Technique to Democratize the Creation of Controllable Morphing 3D Underwater Structures with Low-Cost, Easily Available Hydrogel Beads Adhered to a Substrate. In *Proceedings of the 2021 ACM Designing Interactive Systems Conference* (Virtual Event, USA) (DIS '21). Association for Computing Machinery, New York, NY, USA, 1242–1252. <https://doi.org/10.1145/3461778.3462136>
- Viirj Kan, Emma Vargo, Noa Machover, Hiroshi Ishii, Serena Pan, Weixuan Chen, and Yasuaki Kakehi. 2017. Organic Primitives: Synthesis and Design of pH-Reactive Materials using Molecular I/O for Sensing, Actuation, and Interaction. In *Proceedings of the 2017 CHI Conference on Human Factors in Computing Systems* (Denver, Colorado, USA) (CHI '17). Association for Computing Machinery, New York, NY, USA, 989–1000. <https://doi.org/10.1145/3025453.3025952>
- Mustafa Emre Karagozler, Ivan Poupyrev, Gary K. Fedder, and Yuri Suzuki. 2013. Paper Generators: Harvesting Energy from Touching, Rubbing and Sliding. In *Proceedings of the 26th Annual ACM Symposium on User Interface Software and Technology* (St. Andrews, Scotland, United Kingdom) (UIST '13). Association for Computing Machinery, New York, NY, USA, 23–30. <https://doi.org/10.1145/2501988.2502054>
- Yoshihiro Kawahara, Steve Hodges, Benjamin S. Cook, Cheng Zhang, and Gregory D. Abowd. 2013. Instant Inkjet Circuits: Lab-Based Inkjet Printing to Support Rapid Prototyping of UbiComp Devices. In *Proceedings of the 2013 ACM International Joint Conference on Pervasive and Ubiquitous Computing* (Zurich, Switzerland) (UbiComp '13). Association for Computing Machinery, New York, NY, USA, 363–372. <https://doi.org/10.1145/2493432.2493486>
- Robert J. Lang. 2009. Computational Origami: From Flapping Birds to Space Telescopes. In *Proceedings of the Twenty-Fifth Annual Symposium on Computational Geometry* (Aarhus, Denmark) (SCG '09). Association for Computing Machinery, New York, NY, USA, 159–162. <https://doi.org/10.1145/1542362.1542363>
- Qiyu Lu, Andreea Danelescu, Vikram Iyer, Pedro Lopes, and Lining Yao. 2024. Ecological HCI: Reflection and Future. In *Extended Abstracts of the CHI Conference on Human Factors in Computing Systems* (Honolulu, HI, USA) (CHI EA '24). Association for Computing Machinery, New York, NY, USA, 4 pages. <https://doi.org/10.1145/3613905.3643985>
- Qiyu Lu, Jifei Ou, João Wilbert, André Haben, Haipeng Mi, and Hiroshi Ishii. 2019. MilliMorph – Fluid-Driven Thin Film Shape-Change Materials for Interaction Design. In *Proceedings of the 32nd Annual ACM Symposium on User Interface Software and Technology* (New Orleans, LA, USA) (UIST '19). Association for Computing Machinery, New York, NY, USA, 663–672. <https://doi.org/10.1145/3332165.3347956>
- Qiyu Lu, Danqing Shi, Yingqiang Xu, and Haipeng Mi. 2020. MetaLife: Interactive Installation Based on Liquid Metal Deformable Interfaces. In *Extended Abstracts of the 2020 CHI Conference on Human Factors in Computing Systems* (Honolulu, HI, USA) (CHI EA '20). Association for Computing Machinery, New York, NY, USA, 1–4. <https://doi.org/10.1145/3334480.3383134>
- Qiyu Lu, Haiqing Xu, Yijie Guo, Joey Yu Wang, and Lining Yao. 2023. Fluidic Computation Kit: Towards Electronic-free Shape-changing Interfaces. In *Proceedings of the 2023 CHI Conference on Human Factors in Computing Systems* (Hamburg, Germany) (CHI '23). Association for Computing Machinery, New York, NY, USA, Article 211, 21 pages. <https://doi.org/10.1145/3544548.3580783>
- Qiyu Lu, Tianyu Yu, Semina Yi, Yuran Ding, Haipeng Mi, and Lining Yao. 2023. Sustaininflate: Harvesting, Storing and Utilizing Ambient Energy for Pneumatic Morphing Interfaces. In *Proceedings of the 36th Annual ACM Symposium on User Interface Software and Technology* (San Francisco, CA, USA) (UIST '23). Association for Computing Machinery, New York, NY, USA, Article 32, 20 pages. <https://doi.org/10.1145/3586183.3606721>
- Andres W. Martinez, Scott T. Phillips, George M. Whitesides, and Emanuel Carrilho. 2010. Diagnostics for the Developing World: Microfluidic Paper-Based Analytical Devices. *Analytical Chemistry* 82, 1 (2010), 3–10. <https://doi.org/10.1021/ac9013989> arXiv:<https://doi.org/10.1021/ac9013989> PMID: 2000034.
- Ramsey V. Martinez, Carina R. Fish, Xin Chen, and George M. Whitesides. 2012. Elastomeric Origami: Programmable Paper-Elastomer Composites as Pneumatic Actuators. *Advanced Functional Materials* 22, 7 (2012), 1376–1384. <https://doi.org/10.1002/adfm.201102978> arXiv:<https://onlinelibrary.wiley.com/doi/pdf/10.1002/adfm.201102978>
- Kopyungy (Justin) Moon, Haewon Lee, Jeeeon Kim, and Andrea Bianchi. 2022. ShrinkCells: Localized and Sequential Shape-Changing Actuation of 3D-Printed Objects via Selective Heating. In *Proceedings of the 35th Annual ACM Symposium on User Interface Software and Technology* (Bend, OR, USA) (UIST '22). Association for Computing Machinery, New York, NY, USA, Article 86, 12 pages. <https://doi.org/10.1145/3526113.3545670>
- Koya Narumi, Kazuki Koyama, Kai Suto, Yuta Noma, Hiroki Sato, Tomohiro Tachi, Masaaki Sugimoto, Takeo Igarashi, and Yoshihiro Kawahara. 2023. Inkjet 4D Print: Self-Folding Tessellated Origami Objects by Inkjet UV Printing. *ACM Trans. Graph.* 42, 4, Article 117 (jul 2023), 13 pages. <https://doi.org/10.1145/3592409>
- Ryuuya Niizuma, Xu Sun, Lining Yao, Hiroshi Ishii, Daniela Rus, and Sangbae Kim. 2015. Sticky Actuator: Free-Form Planar Actuators for Animated Objects. In *Proceedings of the Ninth International Conference on Tangible, Embedded, and Embodied Interaction* (Stanford, California, USA) (TEI '15). Association for Computing Machinery, New York, NY, USA, 77–84. <https://doi.org/10.1145/2677199.2680600>
- Masa Ogata and Masaaki Fukumoto. 2015. FluxPaper: Reinventing Paper with Dynamic Actuation Powered by Magnetic Flux. In *Proceedings of the 33rd Annual ACM Conference on Human Factors in Computing Systems* (Seoul, Republic of Korea) (CHI '15). Association for Computing Machinery, New York, NY, USA, 29–38. <https://doi.org/10.1145/2702123.2702516>
- H Okuzaki, T Saido, H Suzuki, Y Hara, and H Yan. 2008. A biomorphic origami actuator fabricated by folding a conducting paper. *Journal of Physics: Conference Series* 127, 1 (aug 2008), 012001. <https://doi.org/10.1088/1742-6596/127/1/012001>

[25] Dinesh K. Patel, Ke Zhong, Haiqing Xu, Mohammad F. Islam, and Lining Yao. 2023. Sustainable Morphing Matter: Design and Engineering Practices. *Advanced Materials Technologies* 8, 23 (2023), 2300678. <https://doi.org/10.1002/admt.202300678> arXiv:<https://onlinelibrary.wiley.com/doi/pdf/10.1002/admt.202300678>

[26] Jie Qi and Leah Buechley. 2012. Animating Paper Using Shape Memory Alloys. In *Proceedings of the SIGCHI Conference on Human Factors in Computing Systems* (Austin, Texas, USA) (CHI '12). Association for Computing Machinery, New York, NY, USA, 749–752. <https://doi.org/10.1145/2207676.2207783>

[27] Christophe Renault, Jessica Koehne, Antonio J. Ricco, and Richard M. Crooks. 2014. Three-Dimensional Wax Patterning of Paper Fluidic Devices. *Langmuir* 30, 23 (2014), 7030–7036. <https://doi.org/10.1021/la501212b> PMID: 24896490. arXiv:<https://doi.org/10.1021/la501212b> PMID: 24896490.

[28] Etienne Reysat and Lakshminarayanan Mahadevan. 2009. Hygromorphs: from pine cones to biomimetic bilayers. *Journal of The Royal Society Interface* 6 (2009), 951 – 957. <https://doi.org/10.1098/rsif.2009.0184>

[29] E. Reysat and L. Mahadevan. 2009. Hygromorphs: from pine cones to biomimetic bilayers. *Journal of The Royal Society Interface* 6, 39 (2009), 951–957. <https://doi.org/10.1098/rsif.2009.0184> arXiv:<https://royalsocietypublishing.org/doi/pdf/10.1098/rsif.2009.0184>

[30] Jihyun Ryu, Maedeh Mohammadifar, Mehdi Tahernia, Ha-ill Chun, Yang Gao, and Seokheun Choi. 2020. Paper Robotics: Self-Folding, Gripping, and Locomotion. *Advanced Materials Technologies* 5, 4 (2020), 1901054. <https://doi.org/10.1002/admt.201901054> arXiv:<https://onlinelibrary.wiley.com/doi/pdf/10.1002/admt.201901054>

[31] Jihyun Ryu, Mehdi Tahernia, Maedeh Mohammadifar, Yang Gao, and Seokheun Choi. 2020. Moisture-Responsive Paper Robotics. *Journal of Microelectromechanical Systems* 29, 5 (Oct 2020), 1049–1053. <https://doi.org/10.1109/JMEMS.2020.2997070>

[32] Danna Tang, Liang Hao, Yan Li, Wei Xiong, Tao Sun, and Xiaokang Yan. 2018. Investigation of wax-based barite slurry and deposition for 3D printing landslide model. *Composites Part A: Applied Science and Manufacturing* 108 (2018), 99–106. <https://doi.org/10.1016/j.compositesa.2018.02.007>

[33] Yutaka Tokuda, Deepak Ranjan Sahoo, Matt Jones, Sriram Subramanian, and Anusha Withana. 2021. Flowcuts: Crafting Tangible and Interactive Electrical Components with Liquid Metal Circuits. In *Proceedings of the Fifteenth International Conference on Tangible, Embedded, and Embodied Interaction* (Salzburg, Austria) (TEI '21). Association for Computing Machinery, New York, NY, USA, Article 35, 11 pages. <https://doi.org/10.1145/3430524.3440654>

[34] Guanyun Wang, Tingyu Cheng, Youngwook Do, Humphrey Yang, Ye Tao, Jianzhe Gu, Byoungkwon An, and Lining Yao. 2018. Printed Paper Actuator: A Low-Cost Reversible Actuation and Sensing Method for Shape Changing Interfaces. In *Proceedings of the 2018 CHI Conference on Human Factors in Computing Systems* (Montreal QC, Canada) (CHI '18). Association for Computing Machinery, New York, NY, USA, 1–12. <https://doi.org/10.1145/3173574.3174143>

[35] Guanyun Wang, Humphrey Yang, Zeyu Yan, Nurcan Gecer Ulu, Ye Tao, Jianzhe Gu, Levent Burak Kara, and Lining Yao. 2018. 4DMesh: 4D Printing Morphing Non-Developable Mesh Surfaces. In *Proceedings of the 31st Annual ACM Symposium on User Interface Software and Technology* (Berlin, Germany) (UIST '18). Association for Computing Machinery, New York, NY, USA, 623–635. <https://doi.org/10.1145/3242587.3242625>

[36] Yihui Wang, Zhongwen Li, Xinyi Huang, Wenbin Ji, Xinghai Ning, Kangkang Liu, Jie Tan, Jiachen Yang, Ho-Pui Ho, and Guanghui Wang. 2019. On-board control of wax valve on active centrifugal microfluidic chip and its application for plasmid DNA extraction. *Microfluidics and Nanofluidics* 23, 10 (Sept. 2019), 112. <https://doi.org/10.1007/s10404-019-2278-y>

[37] Di Wu, Qiuyu Lu, Hsuanju Lai, Yunjia Zhang, and Lining Yao. 2023. Demonstrating Waxpaper Plus: Sequentially and Conditionally Programmable Morphing Wax Fabrics. In *Extended Abstracts of the 2023 CHI Conference on Human Factors in Computing Systems* (Hamburg, Germany) (CHI EA '23). Association for Computing Machinery, New York, NY, USA, Article 442, 5 pages. <https://doi.org/10.1145/3544549.3583924>

[38] Ze Zhao, Youngkyu Hwang, Yun Yang, Tengfei Fan, Juha Song, Subra Suresh, and Nam-Joon Cho. 2020. Actuation and locomotion driven by moisture in paper made with natural pollen. *Proceedings of the National Academy of Sciences* 117, 16 (2020), 8711–8718. <https://doi.org/10.1073/pnas.1922560117> arXiv:<https://www.pnas.org/doi/pdf/10.1073/pnas.1922560117>

[39] Ke Zhong, Adriana Fernandes Minor, Di Wu, Humphrey Yang, Mohammad F. Islam, and Lining Yao. 2023. EpoMemory: Multi-State Shape Memory for Programmable Morphing Interfaces. In *Proceedings of the 2023 CHI Conference on Human Factors in Computing Systems* (Hamburg, Germany) (CHI '23). Association for Computing Machinery, New York, NY, USA, Article 744, 15 pages. <https://doi.org/10.1145/3544548.3580638>

[40] Xiyue Zou, Tongfen Liang, Michael Yang, Cora LoPresti, Smit Shukla, Meriem Akin, Brian T. Weil, Salman Hoque, Emily Gruber, and Aaron D. Mazzeo. 2022. Paper-Based Robotics with Stackable Pneumatic Actuators. *Soft Robotics* 9, 3 (2022), 542–551. <https://doi.org/10.1089/soro.2021.0002> PMID: 34388034. arXiv:<https://doi.org/10.1089/soro.2021.0002> PMID: 34388034.